

# Calorimetry, Structure and Morphology of Printed Samples from Biodegradable Materials Using FDM 3D Printing Technology



Dumitru Nedelcu and Andrei-Danut Mazurchevici

**Abstract** The current concerns of researchers worldwide are focused on the study of top technologies and materials that have minimal impact on life quality. Thus, merging the most used 3D printing technology, FDM-Fused Deposition Modeling, with biodegradable polymeric materials from renewable resources is one of the current topics in the field of industrial research. The aim of the present study is the analysis of FDM printed samples from biodegradable polymers like Extrudr GreenTec Anthracite, Extrudr BDP Pearl, bioFila Linen and bioFila Silk. The used materials for 3D printing, according to the manufacturer and to the obtained results, from morphological investigations point of view, have a high rate of decomposition into chemical elements that are found naturally in nature. The performed analyses were SEM (Scanning Electron Microscopy), EDX—Energy Dispersive X-ray Analysis, XRD—X-Ray Diffraction Analysis and DSC—Differential Scanning Calorimetry analyses in order to identify their elemental composition, the phase transitions suffered by the materials during heating and aspects regarding the adhesion between layers specific to the additive manufacturing. The obtained results support the researchers by providing valuable information that helps to establish some process parameters (melting temperature, printing direction, etc.) but also to understand the materials behavior that take place during the heating process. From a thermal, morphological and structural point of view, 3D printed biodegradable materials can be used in various fields of activity, being able to replace nonbiodegradable polymers that are so harmful to the environment and health.

---

D. Nedelcu (✉) · A.-D. Mazurchevici  
Department of Machine Manufacturing Technology, “Gheorghe Asachi” Technical  
University of Iasi, Blvd. Mangeron, No. 59A, 700050 Iasi, Romania  
e-mail: [dnedelcu@tuiasi.ro](mailto:dnedelcu@tuiasi.ro)

D. Nedelcu  
Academy of Romanian Scientists, Str. Ilfov, Nr. 3, Sector 5, 010164 Bucharest, Romania

© The Author(s), under exclusive license to Springer Nature Switzerland AG 2021  
H. K. Dave and J. P. Davim (eds.), *Fused Deposition Modeling Based 3D Printing*,  
Materials Forming, Machining and Tribology,  
[https://doi.org/10.1007/978-3-030-68024-4\\_3](https://doi.org/10.1007/978-3-030-68024-4_3)

## 1 Introduction

The persistence of fossil fuel based plastics in the environment, the lack of storage space for waste, the concern about emissions during incineration, as well as the dangers of ingestion of these materials have stimulated efforts to develop new biodegradable materials. To be competitive, biodegradable plastics must have properties similar to conventional plastics. Existing biodegradable product lines need to be expanded to meet specific physical requirements and other forms of polymers need to be further researched and modified so that the degradation time varies according to climatic differences and performance requirements. Among the most important factors in the development of a successful biodegradable polymer industry are cost reduction, as well as public and political acceptance [1].

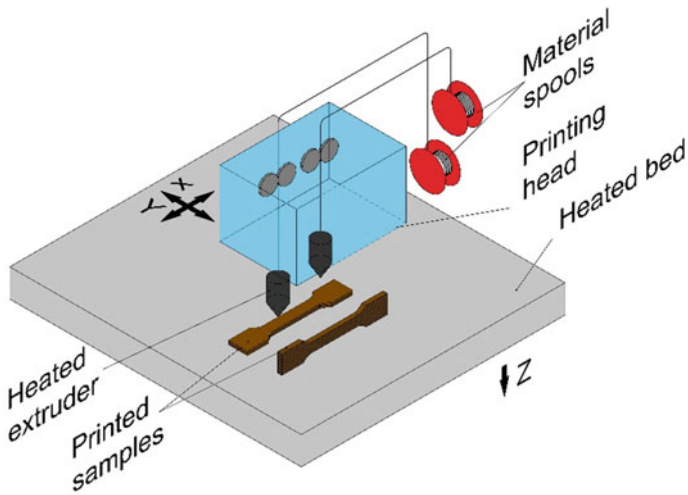
Within the scientific community, it requires the optimization and development of new processes and technologies, which will allow the sustainable production of materials, recyclable, biocompatible and biodegradable, from renewable natural resources. The main challenges in order to convert and obtain industrial materials from bio resources are sustainability, durability, compatibility and accessibility to the new developed materials.

Rapid prototyping is an additive manufacturing technology that determines raw material savings but also the possibility to obtain a prototype in a very short time without the involvement of other conventional processing technologies. The constant need to develop and improve technologies, whether it refers to modern manufacturing technologies or to technologies for obtaining materials with a low impact on the environment, has led to the creation of sustainable products globally [2].

The most widespread technology for obtaining parts by additive manufacturing is Fused Deposition Modeling (FDM), which offers the possibility of obtaining prototypes, of various sizes in a very short time, compared to the possibilities offered by traditional manufacturing technologies, a sketch of this method can be seen in Fig. 1. Parts can be obtained using solid state thermoplastic filaments. The filament is pushed through a heated nozzle where it is melted. The printer continuously moves the nozzle, placing the molten material in precise locations, following a predetermined path. The construction of the part is realised by depositing melted thermoplastic material layer by layer until this one it is completed [2].

The main advantages of FDM technology are: obtaining prototypes in a short time and a low manufacturing cost. However, the technology also has some limitations, among which we mention: low dimensional accuracy for small parts; lower surface quality and lower print speed compared to other printing methods [3]. FDM technology is widely used in various industries for printing parts from the class of electronic enclosures, clamping and fixing devices, injection molds, etc.

Joining the modern technology used for the parts fabrication with the biodegradable materials from renewable resources, leads to obtaining multiple advantages due to the ease of printing biodegradable parts, functional and able to successfully replace conventional plastic ones [3].



**Fig. 1** FDM technology—sketch and model construction

Determining and understanding the functional characteristics of biodegradable materials that can be used in additive manufacturing is essential because only in this manner can be achieved the correct and optimal selection of the material which is thus able to match the application from the targeted field.

In the last decade, due to the need to reduce environmental pollution as a cause of the massive use of exhaustible resources in various industries. Numerous research studies have been conducted on the possibility of replacing polluting materials with biodegradable, compostable or recyclable ones. Thus, 3D printing of biodegradable polymeric materials has been and continues to be a major interest research topic, the biodegradable thermoplastics materials used mainly in FDM printing are PLA (Poly lactic acid) [4–7], PLA-based composite [8–13], PHB—polyhydroxybutyrate [14], PCL—polyhydroxybutyrate [15], lignin based polymers as Arboblend V2 Nature, Arbofill Fichte [16], etc. The results obtained from the carried out studies regarding various properties of 3D printed biodegradable materials certifies the possibility of substituting polymeric materials based on nonbiodegradable resources.

The need of the present paper comes from the total lack of scientific research on the structural and thermal properties of the Extrudr GreenTec Anthracite, Extrudr BDP Pearl, bioFila Linen and bioFila Silk biodegradable materials. So far, no results are known regarding the samples or parts 3D printed from the mentioned materials. Therefore, was necessary the knowledge of these biodegradable thermoplastics characteristics in order to make some recommendations to replace certain parts made from conventional plastics and which are used in spread activity sectors.

## 2 Materials and Methods


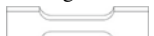
3D printing of the samples required for thermal, structural and morphological determinations was performed using a number of four biodegradable polymeric materials selected according to their usefulness and the possibility of replacing nonbiodegradable synthetic plastics [4, 17]. The biodegradable materials used were Extrudr BDP Green-TEC Anthracite, Extrudr BDP Pearl, bioFila Linen and bioFila Silk.

Extrudr Green-TEC Anthracite and Extrudr BDP Pearl filaments are produced by Extrudr company (Lauterach, Austria). *Extrudr Green-TEC Anthracite* is a BIO performance product (from renewable raw materials—contains PLA—Polylactic acid (based on corn starch, sugar cane or tapioca roots), copolyester and additives) [5], biodegradable according to DIN EN ISO 14855, suitable for applications that require high tensile strength (excellent flexural strength), low deformation and high product surface quality. Also, the material has no smell and is safe for the use industry food. *Extrudr BDP Pearl* is a material 100% from renewable resources, used mainly in applications where the aesthetic part is important (BIO design product) and with mechanical and thermal characteristics comparable to those of PLA. According to the manufacturer its chemical composition is similar to that of Extrudr Green-TEC Anthracite material [18].

The filaments from the purchased bioFila Linen material are totally biodegradable, having higher resistance than other biodegradable materials, it is also characterized by a linen cloth exture, being suitable for projects where the aesthetic part is very important. bioFila Linen is also completely biodegradable, this polymer having a fine and shiny texture reminiscent of silk texture, being ideal for decorations. These two types of filaments are produced by the twoBEars company from Vielank, Germany [19].

3D printing of the samples specific to the tensile test (dumbbell shape—ISO 527 standard) was realised using Raise3D Pro2Plus printing equipment, from the Fine Mechanics and Nanotechnologies Laborator, Faculty of Machine Manufacturing and Industrial Management, “Gheorghe Asachi” Technical University of Iasi. The samples were printed using a 0.4 mm nozzle diameter, 2 or 3 contours (2 for “on edge” orientation and 3 for “flat” orientation) in the shell area—rectilinear type, in the raster area, the set infill type was “grid” but, according to a previous study realized by the research team [20], it was found that for an infilling percentage higher then 95%, the ideaMaker software used by the printing equipment, no longer takes into account the programmer established pattern, automatically switching to the rectilinear pattern. The infilling degree in the raster area was 100%. The rectilinear infilling type results from the superposition of two successive layers in which for the first layer the movement of the printing head is made rectilinearly at an angle of  $+45^\circ$  and for the deposition of the next layer the head movement is also made rectilinearly but in the  $-45^\circ$  direction. There is no movement of the head in the same layer after the grid route. It should also be mentioned that the printing of

**Table 1** Printing parameters used to prototype samples from biodegradable materials

Printing temperatures			Process factors		
Material	<i>Nt</i> (°C)	<i>Pt</i> (°C)	<i>So</i>	<i>Is</i> (mm/s)	<i>Lt</i> (mm)
Extrudr Green-TEC Anthracite	220	60	Flat	40	0.1
Extrudr BDP Pearl	180	55			
bioFila Linen	215	65	On edge	80	0.2
bioFila Silk	220	65			

*Nt* Nozzle temperature, *Pt* Printing bed temperature, *So* sample orientation on the printing bed, *Is* infill speed, *Lt* layer thickness

the samples was performed using a complete factorial experimental plan, the process factors being varied on two levels, Table 1.

For DSC (Differential scanning calorimetry) experiments, tensile test sample fragments of up to 5 mm from all types of materials, with weighing less than 50 mg were cut. For this purpose, a NETZSCH differential scanning calorimeter type DSC 200 F3 Maya was used, with <1 W sensitivity, 0.1 K thermal accuracy and <1% enthalpy accuracy—generally. The equipment has been calibrated according to Bi—Bismut, In—Indium, Sn—Tin and Zn—Zinc standards. Temperature scans were performed between (20–200) °C with a heating rate of 10 K/min, in a Ar—Argon protective atmosphere, the thermal analysis was completed before the samples began to deteriorate, carbonize. The DSC thermograms recorded during heating were evaluated using the Proteus program, provided by NETZSCH using the tangent method. Temperatures were determined where the half of the transformation took place (T50), as well as the amount of heat dissipated or absorbed.

Structural and morphological analysis was performed using SEM and EDX methods on a QUANTA 200 3D electron microscope. For the surface analysis, in order to the realization micrographic maps, samples from the experiments where the highest value of the tensile strength was reached were chosen. The SEM analysis was performed on the surface area of tensile tested samples and for the areas where the complete ruptures occurred, in the cross-section of the samples.

The QUANTA 200 3D electron microscope (also equipped with an EDX detector) was used for SEM (Scanning Electron Microscopy) analysis. The images were obtained taking into account the following parameters: 10–20 kV acceleration voltage of the secondary electrons; 100×–500× magnification power; 15 mm working distance; Large Field Detector (LFD) used for the analysis of non-conductive samples (polymers, textile fibers, powders, etc.); 0° tilt angle; 60 Pa pressure inside the microscope chamber.

X-ray diffraction analysis (XRD) is the most commonly used technique to characterize the crystallinity and phase purity of a material. The X'Pert Pro MRD X-ray diffractometer was used for the X-ray diffractographic analysis. This equipment is equipped with a Cu  $k\alpha$   $\lambda = 1.54 \text{ \AA}$ , Panalytical equipment (Netherlands), to which a 45 kV voltage was applied, the diffraction angle ( $2\theta$ ) varying between 5° and 90° The data obtained were processed using the X'Pert

Data Collector, X'Pert High Score Plus and X'Pert Data Viewer programs, being finally rendered in the diffractograms form in diffraction  $2\theta$  angle coordinates and using the absolute intensity of the maximum diffraction.

### 3 Results and Discussions

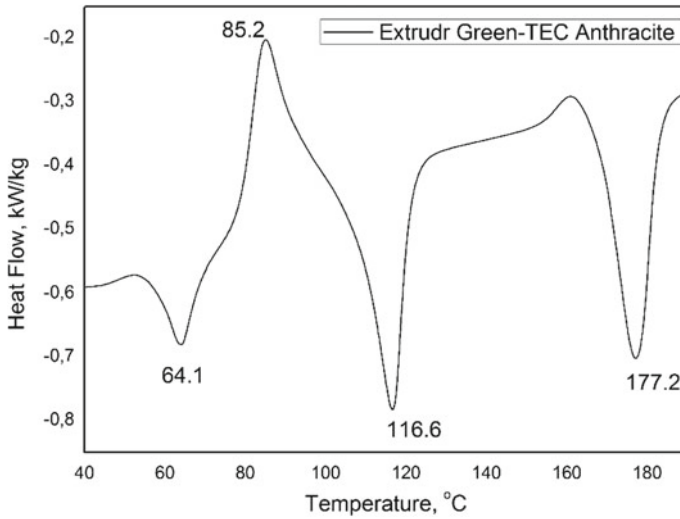
#### 3.1 *Calorimetric Analysis (DSC) for Printed Samples from Biodegradable Materials*

DSC analysis was performed on samples cutted from specific tensile samples printed using the FDM method. The samples printing temperature is an input parameter which in the case of biodegradable polymeric materials printing cannot be varied much, maximum 10–15 °C, considering the own experience accumulated in this field. Thus, our recommendation is to perform a DSC analysis, before starting the printing process, just to see, first of all, the material melting point which can then be correlated with the technical specifications provided by the manufacturer. They generally offer a longer thermal printing range.

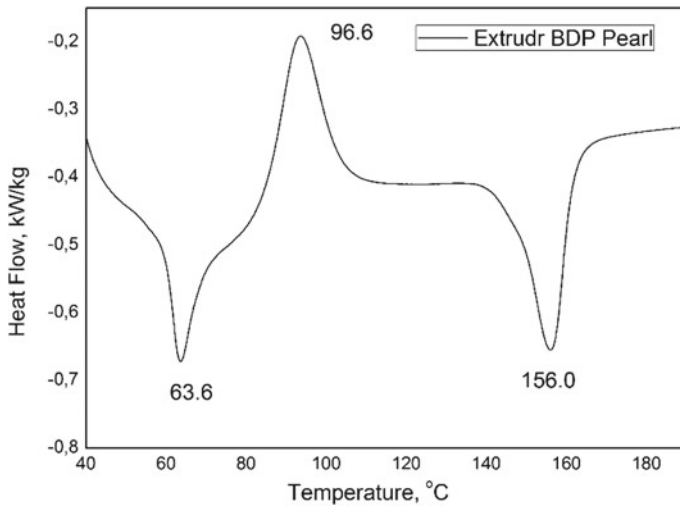
The biodegradable material Extrudr GreenTec Anthracite shows peaks associated with the following phase transitions, Fig. 2: water evaporation from the base matrix (probably lignin) highlighted by an endothermic peak at 64.1 °C, with a quantity of heat absorbed of  $-6.45$  J/g; material crystallization or lignin reorganization (major component of the material structure) at a temperature of 85.2 °C through an exothermic peak, with 18.56 J/g heat release; melting of a constituent element of the biodegradable material highlighted by an endothermic peak at a temperature of 116.6 °C, with a heat consumption of  $-21.6$  J/g; melting point of the material through an endothermic peak at 177.2 °C, with  $-25.43$  J/g amount of heat absorbed.

The printed sample from Extrudr BDP Pearl exhibit after calorimetric analysis three representative peaks, Fig. 3, two endotherms and one exotherm associated as follows: first endothermic peak at 63.6 °C is associated with water evaporation from the base matrix of the material (probably lignin) with heat absorption in the amount of  $-6.92$  J/g; at a temperature of 93.6 °C there is an exothermic peak that corresponds to the material crystallization or can be assigned to a lignin reorganization, a transformation that takes place with 18.53 J/g heat release; at a temperature of 156 °C there is an endothermic peak associated with the melting point of the material and which needed  $-17.43$  J/g to achieve.

The thermal characterization of the biodegradable material bioFila Linen is represented in Fig. 4 which shows two endothermic peaks and an exothermic peak. The endothermic peaks are associated with the water evaporation from the base matrix at a temperature of 63.5 °C ( $-8.63$  J/g absorbed heat) and the melting point of the material at a temperature of 156.6 °C, in the temperature range of (140–165) °C, with the absorption of  $-17.8$  J/g heat. The exothermic peak, at a



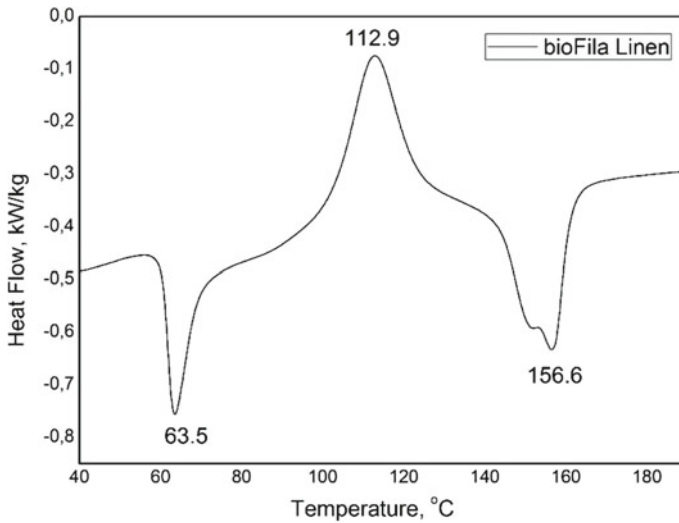
**Fig. 2** Highlighting the main thermal behavior of the printed sample from Extrudr Green-TEC Anthracite



**Fig. 3** Highlighting the main thermal behavior of the printed sample from Extrudr BDP Pearl

temperature of 112.9 °C, corresponds to the material crystallization/a lignin reorganization and takes place with the release of heat in a fairly large amount, 17.97 J/g.

For the biodegradable thermoplastic material bioFila Silk, three peaks, two endotherms and one exotherm were highlighted, corresponding to the following



**Fig. 4** Highlighting the main thermal behavior of the printed sample from bioFila Linen

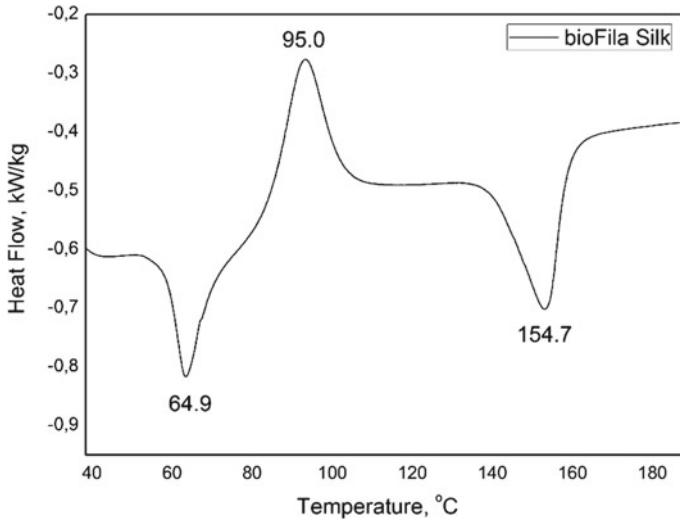
transformations that took place during the heating of the sample up to a temperature of 200 °C, Fig. 5: an endothermic peak at a temperature of 64.9 °C associated with the water evaporation from the base matrix, with heat absorption in the amount of -10.18 J/g; an exothermic peak corresponding to the material crystallization or as well as in the case of the other analyzed materials to a lignin reorganization at a temperature of 95 °C, transformation which took place with heat release, 23.54 J/g; second endothermic peak, at a temperature of 154.7 °C associated to melting point of the bioFila Silk material, with -22.7 J/g heat absorption.

### 3.2 Surface and Structure Analysis for Printed Samples from Biodegradable Materials

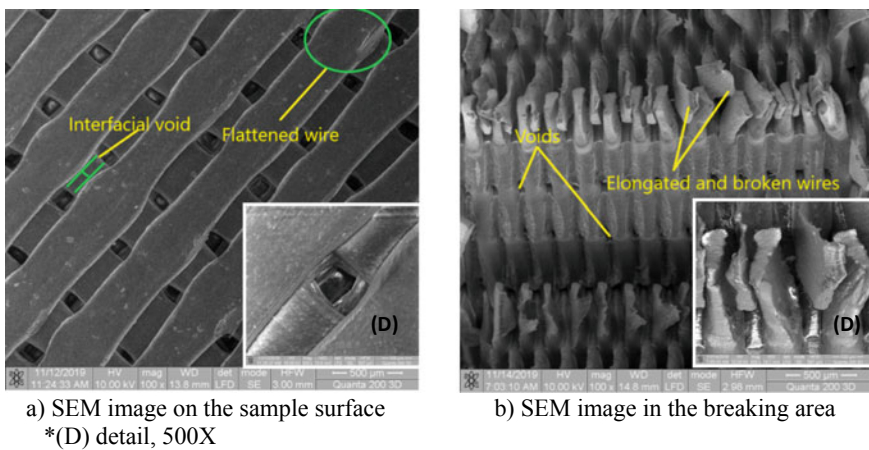
For the surface analysis, in order to realize micrographic maps, tensile tests specific samples were chosen, the SEM analysis being performed for the surface area of the samples and for the area where the complete rupture occurred.

Figure 6 shows the SEM images of the sample from Extruder Green-TEC Anthracite, images in which the slightly uneven profile of the deposited filament can be observed, when making a layer. Due to the nozzle pressure, during printing the melted filament in the upper layer is flattened especially in the area where two filaments on different layers are superimposed, Fig. 6a. In the breaking area, Fig. 6b, reveals a homogeneous structure with filaments specific to printing at +45°/-45°, rectilinear type but also can be observed elongated filaments due to deformation occurred during the tensile test, the material showing breaking filaments





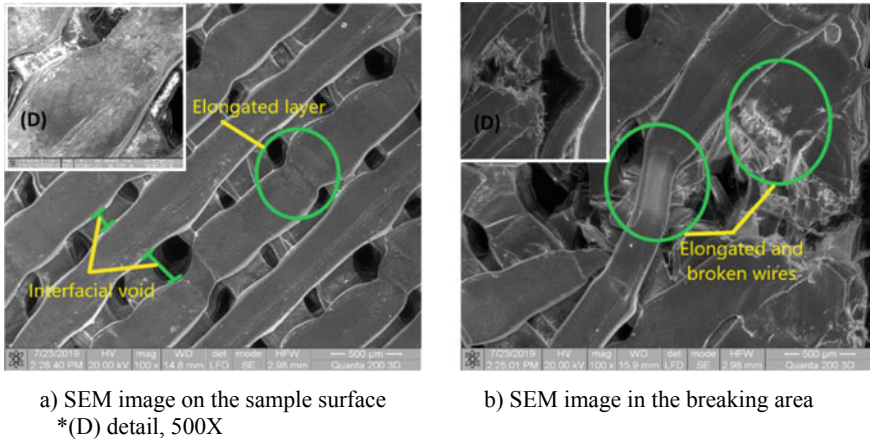
**Fig. 5** Highlighting the main thermal behavior of the printed sample from bioFila Silk



**Fig. 6** SEM images of the printed sample from Extrudr Green-TEC Anthracite, “flat” orientation on the printing bed: **a** SEM image on the sample surface \*(D) detail, 500×, **b** SEM image in the breaking area

specific to elastic polymers. In detail (D), it is observed that in the first phase the outer part of the filament yields, after which the inner, the raster part lengthens until it breaks.

Figure 7a shows the surface structure of the printed sample made of Extrudr BDP Pearl, rectilinear infill pattern, +45°/−45° deposition angle. An uneven profile of the deposited filaments can be observed, when making a layer,



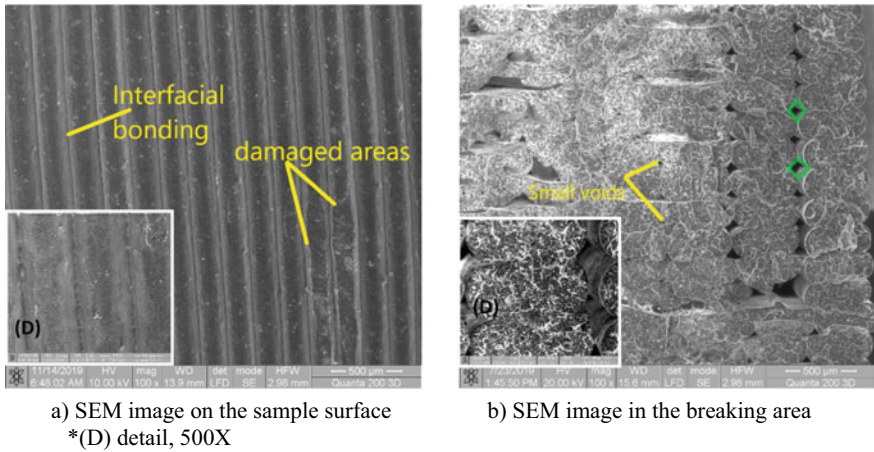
**Fig. 7** SEM images of the printed sample from Extrudr BDP Pearl, “flat” orientation on the printing bed: **a** SEM image on the sample surface \*(D) detail, 500 $\times$ , **b** SEM image in the breaking area

these not being adjacent. It is also possible to observe an almost perfect deposition between the deposited filaments on each layer. There is also a non-uniformity of the extruded filament, filament deformation (detail marked with (D)) in the upper layer more than in the free space created between the deposited filaments. There was also an elongation of the deposited filament in the upper layer due to the space between the deposited filaments on the lower layer, but probably also due to the slow cooling of the deposited filaments.

In the breaking area of the sample, Fig. 7b, there are elongated and broken filaments due to the action of the forces involved in the tensile test. Looking at the figure detail, it can be seen that the filaments breaking is characteristic to ductile materials. Another aspect to be mentioned is that the outer layer of the sample (shell layer) failed first during the test, detaching from the raster area of the sample due to the different structure (printing mode).

In the case of the bioFila Linen material, the surface image of the sample, Fig. 8a, reveals a homogeneous surface with lines specific to the contour area since the sample was printed “on edge” so, the shell area becoming its surface. Damaged areas can also be observed, areas that probably appeared as a result of handling or tensile tests (during sample catching between the tanks).

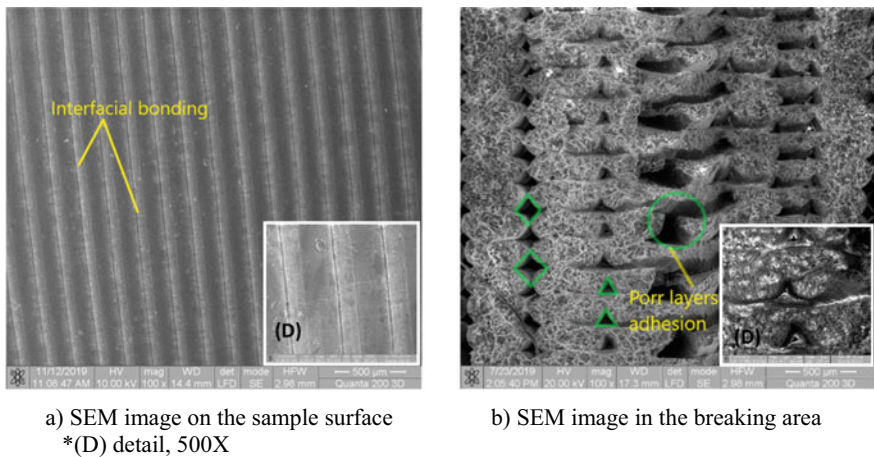
Regarding the analysis of the sample in the breaking zone, Fig. 8b, it was found that the outer shell has a porous structure due to the large size of the rhomboidal voids between the deposited layers. In the raster area the adhesion between the layers is much higher, the porosity decreases a lot. The way the filaments breaks, detail—D, is one specific to rigid materials, behavior also revealed by the specific curves of tensile and bending tests [17].



**Fig. 8** SEM images of the printed sample from bioFila Linen, “on-edge” orientation on the printing bed: **a** SEM image on the sample surface \*(D) detail, 500×, **b** SEM image in the breaking area

For the bioFila Silk material, the surface image of the sample, Fig. 9a, reveals a homogeneous surface with perfectly bonded filaments. At the same time, the adhesion between the extruded and deposited filaments is observed in the detailed image.

For the cross-sectional analysis, Fig. 9b, comparing the size of the triangular gaps in the raster area and the size of the rhomboidal/diamond-shaped gaps in the shell area of the sample was observed contrary to expectations, that in the raster



**Fig. 9** SEM images of te printed sample from bioFila Silk, “on edge” orientation on the printing bed: **a** SEM image on the sample surface \*(D) detail, 500×, **b** SEM image in the breaking area

area the specimen has higher porosity and in some places lack of layers. This inner structure indicates a material rapid cooling, which prevented the extruded filament from filling the free space of the model.

For the samples printed “on edge”, Figs. 8 and 9 the view reveals the layers, one below the other, being the contour, the deposited filaments are perpendicular to the Z direction of the printer, while in the case of “flat” orientation of the sample, Figs. 6 and 7, the view captures the XY plane in which the first layer has the +45° direction, so the SEM images of the surface capturing only this type of layer placement.

Analysing the SEM images of the samples cross-section it can be seen that the *sample orientation on the printing bed* influences their structure and implicitly will influence the provided mechanical responses. Thus, for the samples printed “on edge”, in the raster area the adhesion between the deposited filaments/layers is much compact, Fig. 8b, then in the case of the “flat” printed samples, Fig. 6b. But, the adhesion between the raster area and the shell area is much weaker in the case of “on edge” printing, which is characterized by rather large voids, but which are specific to FDM printing. It should also be taken into account that for “on edge” printed samples the shell percentage is much higher than for “flat” printed specimens, which gives them better mechanical strength because the loading direction and the arrangement direction of the deposited filaments are parallel.

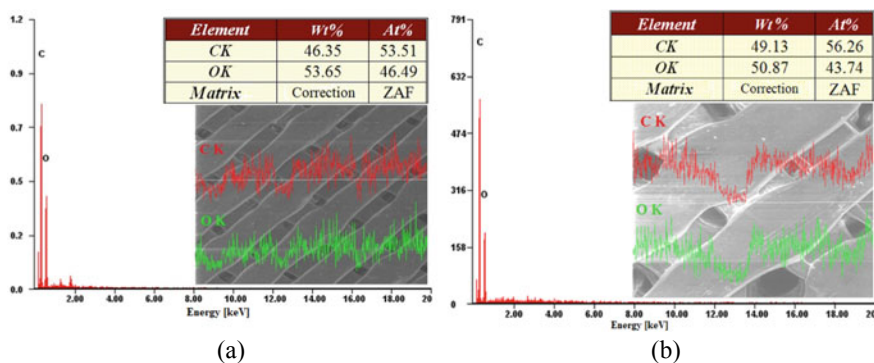
The *layer thickness* influences the mechanical characteristics of the samples but also the surface ones because the thinner the deposited layer is, the higher the sample density and the surface quality will be, Fig. 6 compared to Fig. 7.

The *infill speed* also had a visible influence on the sample from Fig. 7a since compared to Fig. 6a it presents deformed filaments, because during to a layer deposition, the previously deposited filaments fails to solidify completely (being a little thicker) until a new filament is laid. Thus, due to the specific FDM voids and to the filaments weigh, they were deformed.

### ***3.3 EDX Chemical Analysis for Printed Samples Made of Biodegradable Materials***

The following figures show electron microscopy images over which were superimposed line graphs of chemical analysis but also graphs that chemically characterize the printed samples from the studied materials, for experiments with the best results of tensile strength (printed samples).

Figure 10 shows the specific composition highlighted by the prototyped samples from: Extrudr Green-TEC Anthracite and Extrudr BDP Pearl. The main chemical elements identified both in the EDX graph and in the in-line analysis of a portion of the sample were carbon and oxygen in mass and atomic percentages of 54% oxygen, 46% carbon for the Extrudr Green-TEC Anthracite sample and approximately equal proportions of oxygen and carbon for Extrudr BDP Pearl material.



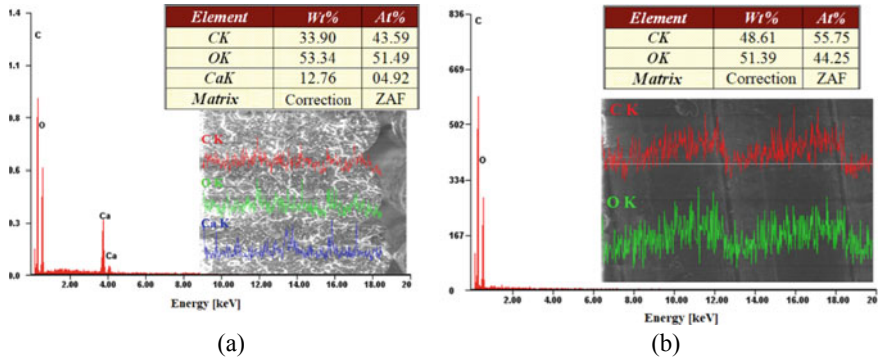
**Fig. 10** EDX spectroscopic analysis for 3D printed materials: **a** Extruder Green-TEC Anthracite, **b** Extruder BDP Pearl

The in-line analysis reflects the structural homogeneity of the printed samples. This analysis also confirms the biodegradable content (biodegradable raw materials—plants) of the materials listed above.

EDX spectroscopic analysis of printed samples from bioFila Linen material, Fig. 11a, and bioFila Silk, Fig. 11b showed that they have in composition similar chemical elements to samples presented above (Extruder Green-TEC Anthracite, Extruder BDP Pearl) but the sample from bioFila Linen has in its mass and atomic composition calcium, in proportion of 12.76% and respectively 4.92%. The presence of calcium could most likely be due to the manufacturer's use of it in order to fine increase the mechanical performance of the material or to reduce the production cost by decreasing the polymer resin amount [21].

In-line EDX analysis in the cross-section of the analyzed samples showed that the materials have a homogeneous structure, with numerous carbon and oxygen bonds.

In-line EDX analyzes, presented in the form of diagrams that are superimposed over the SEM images in the cross section of the filaments, offer the possibility to identify both the constituent elements of the sample and the possibility of locating them. Their location is achieved by tracking the amplitude of the peaks. Thus, for example, in Fig. 11b, it can be easily seen that when the amplitude of the peaks for the carbon distribution diagram (C) is increased, the diagram for oxygen (O) at those points records minimums. This situation is associated with the presence of natural plant fibers that have in their composition a very high amount of carbon. There is also the possibility that the chemical elements have the same amplitude of the peaks for a certain area/point, a case associated with the identification of a carbon-oxygen bond(s).



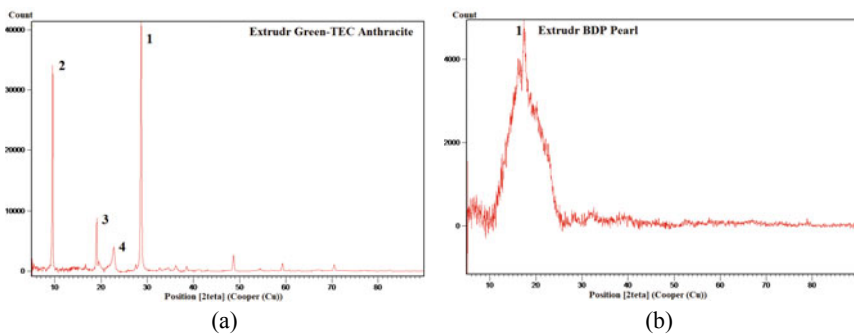
**Fig. 11** EDX spectroscopic analysis for 3D printed materials: **a** bioFila Linen, **b** bioFila Silk

### 3.4 XRD Analysis

XRD analysis, for the study of the materials structure, was used to identify the crystalline phases present in a material and, thus, was revealed information regarding their chemical composition. Phase identification is done by comparing the obtained data with those in the databases reference.

In Fig. 12 are presented the XRD analyzes of Extrudr Green-TEC Anthracite (Fig. 12a) and Extrudr BDP Pearl (Fig. 12b) materials, which reflect their different structure.

The predominant peak noted with 1 for the XRD spectrum of the *Extrudr Green-TEC Anthracite* material is recorded at  $2\theta$  of  $28.68^\circ$  (intensity 41,424) and can be associated with calcium carbonate particles [21, 22], or taking into account that the EDX analysis did not identify calcium element in the chemical composition of the material, another variant would be polyvinyl chloride [23]. For the peak noted by 2 at an angle  $2\theta$  of  $9.5^\circ$  and with an intensity of 34,050, according to the literature



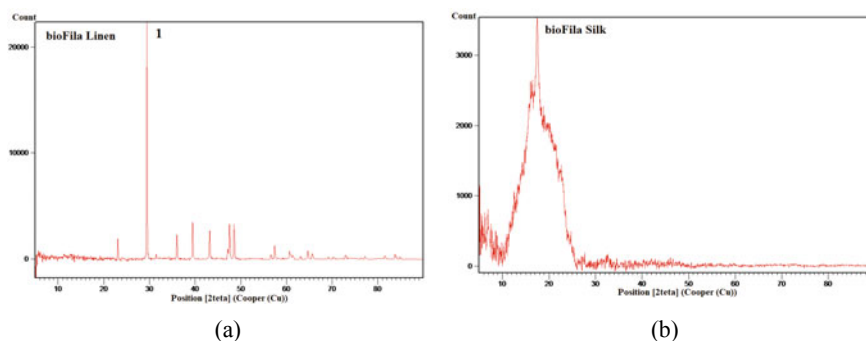
**Fig. 12** XRD analysis for samples printed from: **a** Extrudr Green-TEC Anthracite, **b** Extrudr BDP Pearl

could coincide with the crystallization phase of graphene oxide (GO) [24], which is a biodegradable compound, non-toxic, soluble in water and used in the reinforcement of polymers or composites [25]. There was also a peak, noted with 3, which is similar to that obtained by the authors of the paper [26] at  $19.1^\circ$  angles, intensity 9834, a peak that may be caused by the presence in the composition of lignin or natural fibers. The peak marked with 4 at an angle of  $22.5^\circ$ , corresponds to the area of cellulose crystallization, similar results being obtained by the authors of the papers [27, 28].

The spectrum of *Extrudr BDP Pearl* material shows a major peak, noted by 1, at an angle of  $18.23^\circ$  with a very high intensity (compared to the other studied materials) of 4951. This maximum could be associated with the presence of polyvinylidene fluoride ( $(C_2H_2F_2)_n$ ) known by the acronym PVDF and is used by manufacturers to increase the purity, resistance to solvents, acids and hydrocarbons of the material [29, 30].

The *Extrudr BDP Pearl* material is a semi-crystalline one and the *Extrudr Green-TEC Anthracite* material is a material with a high degree of crystallinity, characterized by narrow peaks and high intensity.

Figure 13 shows the XRD diagrams of the biodegradable materials *bioFila Linen*, Fig. 13a, and *bioFila Silk*, Fig. 13b. The *bioFila Linen* material has a major peak at an angle of  $29.42^\circ$ , noted by 1, at a maximum intensity of 22,417, which according to the authors in references [22, 31] but also to the EDX analysis presented in the previous subsection, may be associated to the calcium carbonate compound ( $CaCO_3$ ). This compound is used by many manufacturers to increase both impact resistance and material rigidity—a requirement that becomes important at high temperatures of use. For example, it is used to make products from PVC (polyvinyl chloride), polypropylene, ABS (Acrylonitrile butadiene styrene) and other ingredients, in order to improve mechanical, electrical and implicitly thermal characteristics such as tensile strength and elongation [21]. Also, the sample from the *bioFillLinen* shows other peaks of much lower intensity which could correspond to the cellulose crystallization [27, 28], polyvinyl chloride or carbon from natural vegetable fibers [26] and others of even lower intensity.



**Fig. 13** XRD analysis for samples printed from: **a** *bioFila Linen*, **b** *bioFila Silk*

The spectrum of the bioFila Silk material shows a maximum diffraction at a  $2\theta$  angle of  $17.47^\circ$  with an absolute intensity of 3547 and which could correspond to polyvinylidene fluoride [29, 30]. The bioFila Linen material is a material with a high degree of crystallinity, but the bioFila Silk material has a semicrystalline structure, being characterized by a wide peak and low intensity compared to the bioFila Linen material.

The rigid behavior of the bioFila Linen material visible in the breaking area of the tensile test specimen (Fig. 8b) is confirmed by the EDX and XRD analyzes which reveal that the material contains calcium carbonate in a percentage of approximately 12%, an additive that confers rigidity to the material [31].

## 4 Conclusions

The calorimetric analysis revealed the thermal behavior of the studied biodegradable materials, thus, identifying specific transitions that took place during a polymer heating: water evaporation from the basic matrices in the first heating part in the case of all samples; crystallizations—which occurs in the case of semicrystalline, crystalline or high crystalline materials and which has also been confirmed by XRD analysis; melting points—necessary to establish the printing temperature but also to observe the materials thermal stability up to the temperature of  $200^\circ\text{C}$ . Another aspect that should be mentioned is the rather low melting point, between  $(154\text{--}176)^\circ\text{C}$  compared to that of synthetic plastics that have melting points above  $200^\circ\text{C}$ , this aspect leading to significant energy reductions during the manufacturing process.

The surface and transversal analyze of the printed samples highlighted their rigid (bioFila Linen and bioFila Silk) or elasto-plastic (Extrudr GreenTec Anthracite and Extrudr BDP Pearl) structure, but also aspects related to the established process parameters, the orientation of the sample on the printing bed having a major influence on the sample physical structure and most likely also on the mechanical characteristics due to the different arrangement of the layers. Infill speed and layer thickness have influenced the surface quality but also the adhesion between the deposited filaments/layers.

EDX and X-ray diffraction analysis highlighted the presence of oxygen and carbon elements (in approximately equal atomic and mass percentages), these ones are found in abundance in plants and annual plant fibers. In the case of bioFila Linen, the material has revealed the presence of calcium carbonate, in a proportion of approximately 13% of the total mass. This filler was used by the manufacturer to fine increase the mechanical performance of this material and to decrease its price with the decrease of the resin amount.

Other information obtained from XRD analysis is closely related to the mechanical responses provided by the printed specimens during the tests reported by the authors of references [4, 17].



Following the performed studies, on the selected biodegradable thermoplastics some recommendations on the possibility of replacing different synthetic polymers in various fields of activity can be done. So, the Extrudr Green-TEC Anthracite, Extrudr BDP Pearl, bioFila Linen, bioFila Silk highlighted a high degree of biodegradability and has thermal, structural, and morphological behavior comparable to that of non-biodegradable polymeric materials, as Acrylonitrile butadiene styrene (ABS), Polyethylene (PET), Polypropylene (PP), Polycarbonate (PC) [32–37], which from this point of view makes them able to substitute the mentioned conventional materials and not only.

**Acknowledgements** This work was supported by a grant of the Romanian Ministry of Research and Innovation, CCCDI—UEFISDI, project number PN-III-P1.2-PCCDI-0446/82PCCDI/2018, acronym TFI PMAIAA/FAMCRIA, within PNCDI III.

## References

1. Pilla S (2011) Engineering applications of bioplastics and biocomposites—an overview, handbook of bioplastics and biocomposites engineering applications. Wiley, New Jersey, pp 1–14
2. Redwood B, Schöffner F, Garret B (2017) The 3D printing handbook technologies, design and applications, Hardcover, pp 24–50
3. Mazurchevici S-N, Mazurchevici A-D, Nedelcu D (2020) Dynamical mechanical and thermal analyses of biodegradable raw materials for additive manufacturing. *Materials* 13:1819. <https://dx.doi.org/10.3390/ma13081819>
4. Mazurchevici A-D, Popa R, Carausu C, Comaneci R, Mazurchevici S-N, Nedelcu D (2020) Basic mechanical analysis of biodegradable materials. In: Paper accepted for publication in proceedings of NewTech2020 international conference, IOP conference series: materials science and engineering
5. Sin LT, Rahmat AR, Rahman WAWA (2012) Polylactic acid: PLA biopolymer technology and applications, 1st ed. Elsevier, Great Britain, pp 22–28
6. CuiFFo MA, Snyder J, Elliott AM, Nicholas Romero N, Kannan S, Halada GP (2017) Impact of the fused deposition (FDM) printing process on polylactic acid (PLA) chemistry and structure. *Appl Sci* 7(6):579. <https://doi.org/10.3390/app7060579>
7. Mazzanti V, Malagutti L, Mollica F (2019) FDM 3D printing of polymers containing natural fillers: a review of their mechanical properties. *Polymers* 11:1094. <https://doi.org/10.3390/polym11071094>
8. van den Oever MJA, Beck B, Müssig J (2010) Agrofibre reinforced poly-(lactic acid) composites: effect of moisture on degradation and mechanical properties. *Compos Part A* 41:1628–1635
9. Gkartzou E, Koumoulos EP, Charitidis CA (2017) Production and 3D printing processing of bio-based thermoplastic filament. *Manuf Rev* 4:2016020
10. Guo R, Ren Z, Bi H, Song Y, Xu M (2018) Effect of toughening agents on the properties of poplar wood flour/poly (lactic acid) composites fabricated with fused deposition modeling. *Eur Polym J* 107:34–45
11. Depuydt D, Balthazar M, Hendrickx K, Six W, Ferraris E, Desplentere F, Ivens J, Van Vuure AW (2019) Production and characterization of bamboo and flax fiber reinforced polylactic acid filaments for fused deposition modeling (FDM). *Polym Compos* 40:1951–1963

12. Liu H, He H, Peng X, Huang B, Li J (2019) Three-dimensional printing of poly (lactic acid) bio-based composites with sugarcane bagasse fiber: effect of printing orientation on tensile performance. *Polym Adv Technol* 30:910–922
13. Stoof D, Pickering K, Zhang Y (2017) Fused deposition modelling of natural fibre/polylactic acid composites. *J Compos Sci* 1:8
14. Vaidya AA, Collet C, Gaugler M, Lloyd-Jones G (2019) Integrating softwood biorefinery lignin into polyhydroxybutyrate composites and application in 3D printing. *Mater Today Commun* 19:286–296
15. Tran TN, Bayer IS, Heredia-Guerrero JA, Frugone M, Lagomarsino M, Maggio F, Athanassiou A (2017) Cocoa shell waste biofilaments for 3D printing applications. *Macromol Mater Eng* 302:1700219
16. Mazurchevici S-N, Mazurchevici A-D, Nedelcu D (2020) Dynamical mechanical and thermal analyses of biodegradable raw materials for additive manufacturing. *Materials* 13:1819. <https://doi.org/10.3390/ma13081819>
17. Carausu C, Mazurchevici S-N, Mazurchevici A-D, Andrusca L, Comaneci R, Popa R, Nedelcu D (2020) mechanical characterization of additive manufactured samples from biodegradable materials. In: Paper accepted for publication in proceedings of ModTech2020 international conference, IOP conference series: materials science and engineering
18. Extrudr. <https://www.extrudr.com/en>. Accessed 09 Nov 2019
19. Two-bears. <http://www.two-bears.eu>. Accessed 09 Nov 2019
20. Mazurchevici A-D, Carausu C, Ciofu C, Popa R, Mazurchevici S-N, Nedelcu D (2019) Infill and type influence on tensile strength of pla biodegradable material using FDM technology. *Int J Modern Manuf Technol* XI 2:44–49
21. Plastic technology. <https://www.ptonline.com/knowledgecenter/plastics-feeding/application-profiles>. Accessed 09 Nov 2019
22. Facchinetto SE, Bortolotto T, Neumann GE, Vieira JCB, de Menezes BB, Giacomelli C, Vanessa Schmidt V (2017) Synthesis of submicrometer calcium carbonate particles from inorganic salts using linear polymers as crystallization modifiers. *J Braz Chem Soc* 28 (4):547–556
23. Wankasi D, Dikio E D (2014) Polyvinyl chloride waste as an adsorbent for the sorption of  $Pb^{2+}$  from aqueous solution. *J Chem* 817527. <https://dx.doi.org/10.1155/2014/817527>
24. Vargas LR, Poli AK, de Cássia Lazzarini Dutra R, de Souza CB, Ribeiro Baldan M, Gonçalves ES (2017) Formation of composite polyaniline and graphene oxide by physical mixture method. *J Aerosp Technol Manag São José dos Campos* 9(5 1):29–38
25. Hielscher ultrasunete tehnologie. <https://www.hielscher.com/ro/graphene-oxide-ultrasonic-exfoliation-and-dispersion.htm>. Accessed 09 Nov 2019
26. Wu C-S (2004) Analysis of mechanical, thermal, and morphological behavior of polycaprolactone/wood flour blends. *J Appl Polymer Sci* 94:1000–1006. <https://dx.doi.org/10.1002/app.20837>
27. Poletto M, Ornaghi Júnior HL, Zattera AJ (2014) Native cellulose: structure, characterization and thermal properties. *Materials* 7:6105–6119. <https://dx.doi.org/10.3390/ma7096105>
28. Kaushik VK, Kumar A, Kalia S (2012) Effect of mercerization and benzoyl peroxide treatment on morphology, thermal stability and crystallinity of sisal fibers. *Int J Textile Sci I* (6):101–105. <https://dx.doi.org/10.5923/j.textile.20120106.07>
29. Cai Xiaomei, Lei Tingping, Sund Daoheng, Linde Liwei (2017) A critical analysis of the a, b and g phases in poly (vinylidene fluoride) using FTIR. *RSC Adv* 7:15382
30. Janakiraman S, Surendran Abhijith, Ghosh Sudipto, Anandhan S, Venimadhav A (2016) Electroactive poly (vinylidene fluoride) fluoride separator for sodium ion battery with high coulombic efficiency. *Solid State Ionics* 292:130–135
31. Helmia FM, Elmitwallib HR, Elnagdy SM, El-Hagrassy AF (2016) Calcium carbonate precipitation induced by ureolytic bacteria *Bacillus licheniformis*. *Ecol Eng* 90:367–371. <https://doi.org/10.1016/j.ecoleng.2016.01.044>
32. Trhliková L, Zmeskal O, Psencik P, Florian P (2016) Study of the thermal properties of filaments for 3D printing. *AIP Conf Proc* 1752:040027. <https://doi.org/10.1063/1.4955258>

33. Elkholy A, Rouby M, Kempers R (2019) Characterization of the anisotropic thermal conductivity of additively manufactured components by fused filament fabrication. *Progress Addit Manuf* 4:497–515
34. Ngo Ich-Long, Jeon Sangwoo, Byon Chan (2016) Thermal conductivity of transparent and flexible polymers containing fillers: a literature review. *Int J Heat Mass Transf* 98:219–226. <https://doi.org/10.1016/j.ijheatmasstransfer.2016.02.082>
35. Garzon-Hernandez S, Garcia-Gonzalez D, Jérusalem A, Arias A (2019) Design of FDM 3D printed polymers: an experimental-modelling methodology for the prediction of mechanical properties. *Mater Des* 188:108414. <https://doi.org/10.1016/j.matdes.2019.108414>
36. Abeykoon C, Sri-Amphorn P, Fernando A (2020) Optimization of fused deposition modeling parameters for improved PLA and ABS 3D printed structures. *Int J Lightweight Mater Manuf* 3(3):284–297. <https://doi.org/10.1016/j.ijlmm.2020.03.003>
37. Wojtyła S, Klama P, Baran T (2017) Is 3D printing safe? Analysis of the thermal treatment of thermoplastics: ABS, PLA, PET, and nylon. *J Occup Environ Hyg* 14(6):D80–D85. <https://doi.org/10.1080/15459624.2017.1285489>